



Regular article

In situ nanobeam electron diffraction strain mapping of planar slip in stainless steel

Thomas C. Pekin^{a, b, *}, Christoph Gammer^c, Jim Ciston^b, Colin Ophus^b, Andrew M. Minor^{a, b, *}^a Department of Materials Science and Engineering, University of California, Berkeley, Berkeley 94720, USA^b National Center for Electron Microscopy, Molecular Foundry, Lawrence Berkeley National Laboratory, Berkeley 94720, USA^c Erich Schmid Institute of Materials Science, Austrian Academy of Sciences, Jahnstrasse 12, Leoben 8700, Austria

ARTICLE INFO

Article history:

Received 7 September 2017

Received in revised form 3 November 2017

Accepted 4 November 2017

Available online xxxx

Keywords:

Nanobeam electron diffraction

Strain measurement

Scanning/transmission electron microscopy

Planar slip

ABSTRACT

Nanobeam electron diffraction strain mapping has been used to measure the strain evolution in stainless steel under in situ deformation. As the amount of deformation increases, the leading dislocation of a planar slip band leaves behind a residual strain in the form of a small lattice expansion. Dislocation analysis confirmed that the dislocations involved were $\langle 011 \rangle$ type. While the characteristic residual strain of planar slip has often been observed, it has never before been directly measured. Our results provide a view into the dynamic mechanisms of planar slip, and showcase the possibilities of multidimensional in situ imaging.

Published by Elsevier Ltd on behalf of Acta Materialia Inc.

The deformation of crystalline materials is highly dependent on defects and their response to applied stress [1,2]. Understanding the motion and dynamic response of these defects, as well as their interactions with each other, is key to future alloy development. A new tool for quantifiably probing these interactions over a large area is scanning nanobeam electron diffraction (NBED). NBED [3–7] is a scanning transmission electron microscopy (STEM) technique that allows for the quantification of strain fields around features of interest at the level of single nanometers. This method, which utilizes a semi-converged electron beam, is faster than methods utilizing electron beam precession [7–9], and can acquire a larger field of view when compared to methods requiring atomic resolution [6,9,10]. Additionally, while NBED requires a sample close to a zone axis, it is relatively robust to imperfect sample tilt, which is all but guaranteed during an in situ deformation experiment [6]. This combination of speed, robustness to sample orientation [11], and increased field of view has allowed for the development of in situ strain mapping, in which the sample is mechanically deformed while successive strain maps are acquired [12]. While traditional TEM based in situ mechanical testing has been a useful technique in understanding

the mechanisms of deformation [13,14], by combining nanoscale deformation with simultaneous strain mapping, we now acquire quantitative data on the local strain field evolution and its relationship with dislocation motion.

It is generally known that the dislocation slip character can be classified in one of two ways [15]. Typically, dislocations either move in three dimensions via wavy slip, or in two-dimensional oriented ensembles known as planar slip [16]. There is a wide body of both experimental and theoretical literature that has shown that the dislocation slip character has a large effect on the resulting mechanical properties of the material, including fracture behavior, fatigue resistance, and stress corrosion cracking [17–24]. In close packed materials (both face-centered cubic (FCC), and hexagonal (HCP)), the presence of short range order (SRO) has been found to be the main factor leading to planar slip [16,25,26].

Planar slip features can be readily observed in lightly deformed stainless steels, as shown in Fig. 1. Fig. 1a is a TEM bright field micrograph of a single instance of planar slip showing multiple dislocations. Fig. 1b is an ADF STEM image showing the long range and regular orientation of these defects.

In alloys containing SRO, planar slip begins when the leading dislocation moves through the matrix, and as it moves, shifts the lattice by a Burgers vector, **b**. This is thought to lead to the local destruction of the SRO, as the locally ordered atoms are shifted out of their energetically favorable positions into a more disordered state. The result of this shift is glide plane softening, which allows further

* Corresponding authors at: Department of Materials Science and Engineering, University of California, Berkeley, Berkeley 94720, USA.

E-mail addresses: tcpekin@berkeley.edu (T.C. Pekin), aminor@berkeley.edu (A.M. Minor).

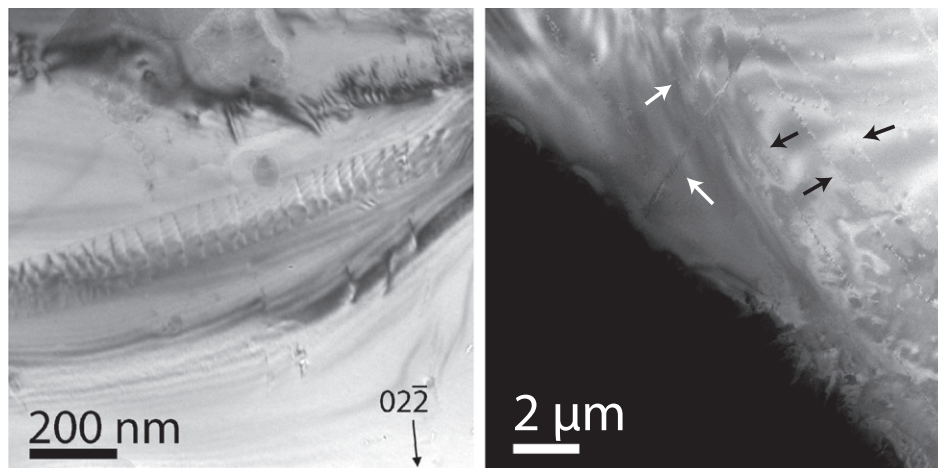


Fig. 1. a) A bright field TEM image of a single instance of planar slip in 321 stainless steel. Note the orderly array of dislocations. b) An ADF STEM image of the same alloy at a lower magnification. Multiple large arrays of planar slip can be seen oriented along specific crystalline directions. Arrows highlight the location of a few of the more prominent examples.

dislocations to move more easily if they follow the first, thereby forming characteristic planar slip bands [16,26]. These highly local, heavily disordered regions then have a deleterious effect on macroscopic mechanical properties due to the resulting stress concentrations as opposed to alloys with more homogeneous wavy slip.

In this experiment, a AISI 321 FCC austenitic stainless steel was pulled in tension in situ in a TEM using a Gatan 654 straining holder. To accurately determine composition, samples were sent to Luvak Inc. for analysis. To determine the majority of the elements in the foil, direct current plasma emission spectroscopy was used [27]. Inert gas fusion was used to determine nitrogen composition [28], and combustion infrared detection was used to determine carbon composition [29]. The composition is shown in Table 1. The as rolled foil was electrical discharge machined (EDM) into 11 mm by 2.5 mm blanks, annealed at 1060 °C for 30 min to anneal out many of the dislocations, and then jet polished to electron transparency using a solution of 6% perchloric acid, 39% butanol and 55% methanol at –15 °C and approximately 30 V. The scanning NBED was performed on the TEAM 1 microscope which is double aberration corrected, and the diffraction patterns were acquired using the Gatan K2 IS electron detector at 400 frames per second. The microscope was operated at 300 kV, with a convergence angle of 2.62 mrad and a camera length of 230 mm, resulting in a collection angle of 32–160 mrad. Eight loading steps were applied. As the Gatan 654 holder does not measure load or accurate displacement, the tensile bar was elongated until dislocation motion commenced. Loading was then paused and a 100 by 100 pixel NBED map with a 2.2 nm step size was acquired. At 400 frames per second, each map took 25 s. Post-deformation ex situ dislocation characterization was performed on the same sample, but in a different region as the in situ region was destroyed during the in situ test. The dislocation characterization was performed on a JEOL 3010 TEM at 300 kV, and the dislocations were found to be [011] type perfect dislocations, as were all dislocations analyzed in similarly prepared samples. The strain mapping analysis was processed using MATLAB, using the hybrid method detailed in [11]. The reference lattice chosen was the mean diffraction pattern for each frame, resulting in a map showing the deviation from the mean strain at each discretely applied load. Post-processing included cropping

to remove exceptionally noisy areas and smoothing. The smoothing was applied using the VBM4D MATLAB package [30], which is optimized for video data.

The results (full video available online in Supplementary materials) can be seen in Fig. 2. Three discrete time-steps are shown, with a, e and i showing the annular dark field (ADF) images acquired simultaneously at each step. Several features can be seen in the ADF images, including a strong bend contour, several dislocations, and a circular precipitate used as a reference for aligning the video frames. However, only one dislocation is caught moving in the field of view from left to right. This is the top dislocation in the image, and it moves a small amount from a to e, while in i it has fully propagated across the field of view. The white arrows denote the location of the leading dislocation. As the dislocation moves, it leaves behind a region of increased contrast in the ADF images. This region of higher contrast matches the band directly beneath it, which was observed previously in the same experiment to be another instance of planar slip in parallel with the moving dislocation shown here.

Strain maps are also shown in Fig. 2. The maps are rather complex as we are measuring the transient strains around multiple dislocations and precipitates in situ. Examining the evolution of strain with respect to deformation, there are some very interesting observations. As the leading dislocation of planar slip moves from left to right, the strain in the 200 direction increases behind it. However, in the perpendicular 022 direction, strain remains constant, showing clear directionality when it comes to the lattice expansion. The evolution during loading of the lattice expansion $((\epsilon_{200} + \epsilon_{022})/2)$ is shown in Fig. 2d, h, and l. Color coded line profiles (10 pixel integration width) from between the arrows in the expansion maps are shown in sub-panel n. While the consistent large dips in the line profiles are due to deleterious effects of sample bending during strain mapping analysis, the profiles reveal that in the second loading step, there is a small lattice expansion as the dislocation moves from left to right, and then at the final loading step, the entire profile is shifted up roughly 0.15%. This corresponds to lattice expansion of 0.3%. This small, directional lattice expansion is not unexpected. In fact, when observing planar slip with standard TEM techniques, it is somewhat characteristic of planar slip to leave behind weak fringing. While we do not see the fringing in our ADF images during strain mapping due to the zone axis imaging condition, we can see them in Fig. 3, which is a representative ex situ 2-beam TEM image of a similar planar slip band from an intact region after releasing the tensile load for deformation.

The weak fringing observed in Fig. 3 is another manifestation of the residual displacement or strain that was observed behind the first

Table 1
The alloy composition as tested.

Element	Fe	Cr	Ni	Mn	Si	Ti	C	N
wt%	Bal.	17.74	9.25	1.71	0.53	0.33	0.031	0.018

Download English Version:

<https://daneshyari.com/en/article/7911236>

Download Persian Version:

<https://daneshyari.com/article/7911236>

[Daneshyari.com](https://daneshyari.com)